Numerical analysis of the mechanical behavior of welded I beam-to-RHS column connections

Rosicley J. R. Rosa[*] and Juliano G. R. Neto[a]

Department of Civil Engineering, Pontifical Catholic University of Goiás,
Av. Universitária 1.440, Setor Universitário, Goiânia, Goiás, Brazil

Abstract. Considering the increasing use of tubular profiles in civil construction, this paper highlights the study on the behavior of welded connections between square hollow section column and I-beam, with emphasis on the assessment of the joint stiffness. Firstly, a theoretical analysis of the welded joints has been done focusing on prescriptions of the technical literature for the types of geometries mentioned. Then, a numerical analysis of the proposed joints were performed by the finite element method (FEM) with the software ANSYS 16.0. In this study, two models were evaluated for different parameters, such as the thickness of the cross section of the column and the sizes of cross section of the beams. The first model describes a connection in which one beam is connected to the column in a unique bending plane, while the second model describes a connection of two beams to the column in two bending planes. From the numerical results, the bending moment-rotation (M-φ) curve was plotted in order to determine the resistant bending moment and classify each connection according to its rotational capacity. Furthermore, an equation was established with the aim of estimating the rotational stiffness of welded I beam-to-RHS column connections, which can be used during the structure design. The results show that most of the connections are semi-rigid, highlighting the importance of considering the stiffness of the connections in the structure design.

Keywords: steel structures; hollow section column; welded connections; bending moment-rotation

1. Introduction

The increasing use of steel structures is associated with advantageous factors in relation to reinforced concrete structures, highlighting: the upper productivity, the possibility of building structures with longer spans using lighter elements, the high precision of the parts and joints of the structures and the possibility of reusing.

The tubular sections (circular hollow sections CHS and rectangular hollow sections RHS, including square ones) have been highlighted among the steel structures, because these sections provide the most efficient use of a steel cross section in resisting compression, tension, bi-axial bending and torsion (Lu 1997).

The growing demand for the hollow sections in civil construction is related to the several

---

[*]Corresponding author, Undergraduate, E-mail: rosicley.eng@outlook.com
[a]Ph.D., E-mail: julianogeraldo.puc@gmail.com
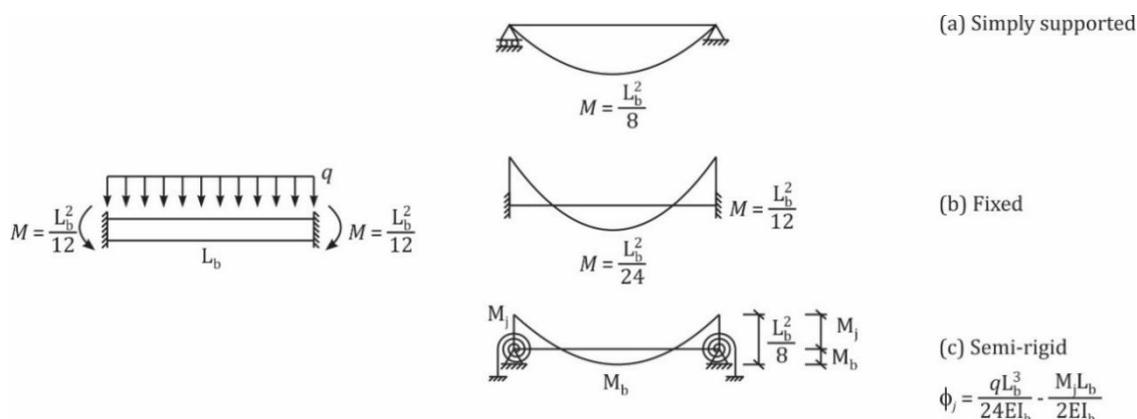
Fig. 1 Beam with various end conditions (adapted from CIDECT 2010)

possibilities of use; and according Matos *et al* (2015), this is justified basically due to their mechanical and aesthetical characteristics. For example, the hollow section can be combined with concrete, in order to increase the compressive strength and to provide fire protection. The Comité International pour le Développement et l'Etude de la Construction Tubulaire (CIDECT 2010) points out that the reinforced concrete filled hollow section columns without external fire protection can reach a fire life of even 2 hours depending on the cross section ratio of the steel and concrete.

Díaz *et al.* (2011) highlights that during the development of a structural project, it is necessary to consider not only the capacity of the insulated elements, but also the structure as a whole. Moreover, it is necessary to analyze the behavior of the joints between two or more profiles. In this sense, Matos *et al.* (2015) comment that the available analytical formulations to predict the behavior of hollow sections have been included in recent design codes, such as Eurocode 3 (EN 1993-1-8 2005) and, more recently, the Brazilian ABNT NBR 16239 (2013) code. Thus, the elements must be chosen strategically, so that to develop a structural project with the adequate joints and lower cost during the constructive process. In this sense, suitable and accurate design methods plays and important role in design of systems which employs hollow sections because they affect the cost and the safety of the structure as explained by Matos *et al.* (2015).

Machado (2013) states that the types of joint have a strong influence on the structural system, since there are many ways to connect beams and columns. The joints are able to generate geometric discontinuities, changing the linear behavior of the structure. In this research, the joints between I-beams and square hollow section columns will be done through welding, because this type of joint is simpler to represent the behavior of a rigid joint between sections of different geometries.

According to Faridmehr *et al.* (2016), in analysis and design of steel frame structures, the connections are considered in two extreme cases in relation to their mechanical behavior. One of these extremes is known as rigid connection while the other one is referred to as pinned connection. In the first, in case of bending moment resistant connections, there is no relative rotation after the deformation of the structure. On the other hand, the pinned connections have opposite behavior, because they do not restrict the relative rotation during the deformation process. Nevertheless, as presented by Lozano *et al* (2018), the beam-column joints usually behave as semi-rigid, which means the beam transmits bending moment to the column proportionally to its

stiffness.

The semi-rigid connections enable the development of a structural design using slender sections due to the lower design bending moment when compared to a rigid or pinned connection, as it can be seen in Fig. 1. Nunes (2012, *apud* CIDECT 2010) states that the use of these connections in a framed structure can reduce the cost from 10% to 20%.

Studies involving RHS columns and I-beams were presented by Lu (1997), CIDECT (2010), Nunes (2012), Guerra *et al.* (2013), Wu and Feng (2013), Serrano-López *et al.* (2016), Eslami and Namba (2016a), Eslami and Namba (2016b) among others. In order to continuing the studies on the RHS steel connections, this paper reports the results of theoretical and numerical analysis of welded joints. The theoretical analysis is based on the prescription of Lu (1997) and CIDECT (2010). The numerical analysis of the joints was performed by the Finite Element Method (FEM) with the software ANSYS 16.0.

This paper aims to study the mechanical behavior of uniplanar and multiplanar welded connections between square hollow section column and I beam. It, specifically, aims to determine the resistant bending moment, plot the M-φ curve and classify the connections according to its rotational capacity. Since Eurocode 3 (EN 1993-1-8 2005) and CIDECT (2010) do not have a tool to determine the connection stiffness, an equation was proposed to estimate the rotational stiffness of welded I beam-to-RHS column connections, which enables the consideration of the connections stiffness in the structure design, in order to obtain projects with lower costs.

2. Theoretical analysis

2.1 Stiffness classification of the connections

The moment-rotation curve indicates the behavior of the welded connections due to the possibility to classify these connections and determine the resistant moment and the rotation capacity. The joint stiffness is equivalent to the tangent in the linear stretch of the curve. In order to classify the joints, Eurocode 3 (EN 1993-1-8 2005) provides stiffness classification, as shown in Fig. 2, in which $S_{j,ini}$ is the joint stiffness, E is the elasticity modulus of the steel, I_b and L_b are, respectively, the moment of inertia and the length of the beam. In this study, the moment-rotation is determined by numerical simulation using the software ANSYS 16.0.
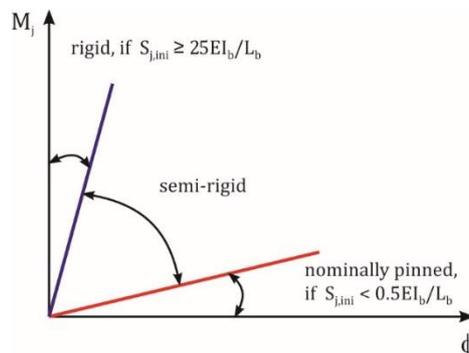

Fig. 2 Limits for stiffness classification of beam-to-column joints for unbraced frames (adapted from Eurocode 3-EN 1993-1-8 2005)

2.2 Failure mode

The CIDECT (2010) proposes seven failure modes involving welded I beam-to-RHS column joints. The sizing of the connections is done according to the failure mode that it is subjected. Furthermore, the failure modes, which must be considered for design, are: the local failure of the beam flange, the column plastification (face, wall or cross section), the column punching shear and the column shear failure. The failure mode predicted for the models of this research, as well as predicted in the studies of Rocha and Neto (2016), is the column wall plastification, which is represented by Eqs. (1) and (2) proposed respectively by CIDECT (2010) and Lu (1997) and illustrated in Fig. 3.

$$M_{1,Rd} = f_{y0}t^2{}_0 \left(\frac{4}{\sqrt{1-\beta}} \right)(h_1 - t_1) \tag{1}$$

$$M_{1,Rd} = f_{y0}t^2{}_0(h_1 - t_1) \left(\frac{2}{\sqrt{1-\beta}} + \frac{1}{2\eta} + \frac{\eta}{1-\beta} \right) \tag{2}$$

In Eqs. (1) and (2) $M_{1,Rd}$ is the design resistant bending moment, f_{y0} is the yield stress of the RHS member, t_0 is the wall thickness of the column, h_1 is the depth of the I section, t_1 is the flange thickness of the I beam. In addition, the important geometric parameters (β, 2γ and η) are presented in the following equations being b_1 the width of the I-beam and b_0 the width of the RHS column.

$$\beta = \frac{b_1}{b_0} \tag{3}$$

$$2\gamma = \frac{b_0}{t_0} \tag{4}$$

$$\eta = \frac{h_1}{b_0} \tag{5}$$
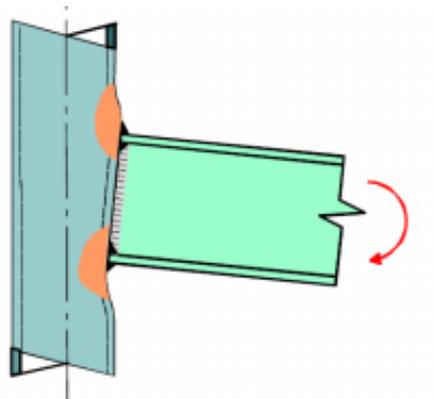
Fig. 3 Column wall plastification (adapted from CIDECT 2010)

3. Numerical analysis

The most suitable and accurate methodology to determine the connection behavior is through experimental analysis, which is very expensive for design practices, being restricted only in researches. So, to overcome this inconvenient, computational simulation can be performed to predict the M-φ curve considering (as desirable) the non-linear behavior. In this study, numerical analyses of uniplanar and multiplanar joints were carried out by the Finite Element Method (FEM) with the software ANSYS 16.0, as shown in Fig. 4.

| (a) | (b) |
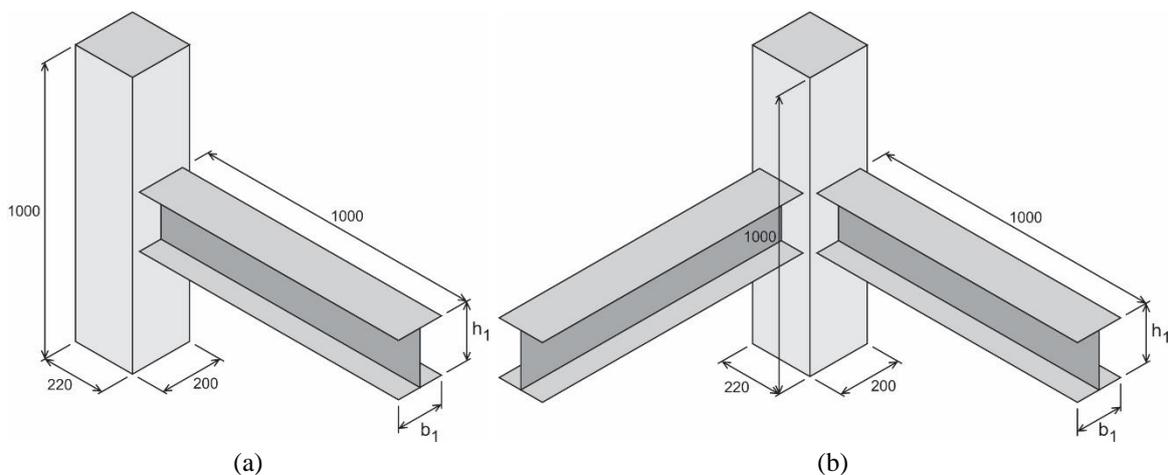
Fig. 4 Geometry and sizes of (a) uniplanar model; (b) multiplanar model. Units in mm

The models were developed with one or two I-beams and a square hollow section column. These elements contain 1000 mm in length. Some combinations of the geometric parameters b_0, t_0, h_1, b_1, t_w and t_f were evaluated, being these combinations given in Table 1.

Table 1 Developed models

| Uniplanar Model | Multiplanar Model | Column | I-beam | Dimensions (mm) | | | | | |
| | | | | Column | | | I-beam | | |
				b_0	t_0	h_1	b_1	t_w	t_f
M1-U	M1-M	220x220x10	W200x15.0	220	10	200	100	4.3	5.2
M2-U	M2-M	220x220x10	W200x26.6	220	10	207	133	5.8	8.4
M3-U	M3-M	220x220x10	W200x41.7	220	10	205	166	7.2	11.8
M4-U	M4-M	220x220x16	W200x15.0	220	16	200	100	4.3	5.2
M5-U	M5-M	220x220x16	W200x26.6	220	16	207	133	5.8	8.4
M6-U	M6-M	220x220x16	W200x41.7	220	16	205	166	7.2	11.8
M7-U	M7-M	220x220x20	W200x15.0	220	20	200	100	4.3	5.2
M8-U	M8-M	220x220x20	W200x26.6	220	20	207	133	5.8	8.4
M9-U	M9-M	220x220x20	W200x41.7	220	20	205	166	7.2	11.8
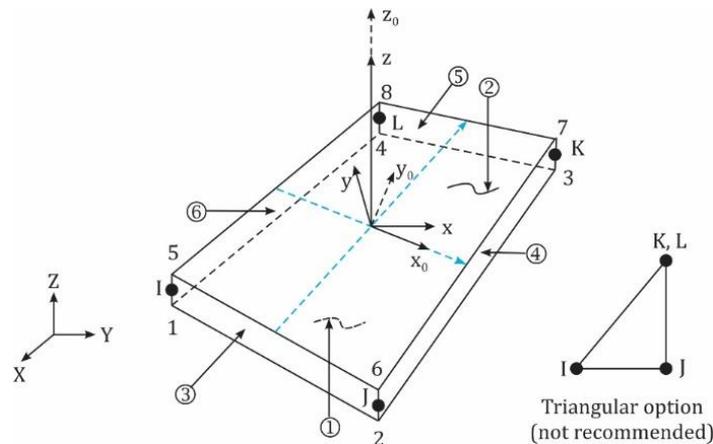
Fig. 5 SHELL181 element (adapted of ANSYS 16.0 2015)

Model adapted from Maggi (2004)

| Point	Strain	Stress
1	1.725×10^{-3}	345.0
2	1.552×10^{-2}	345.0
3	3.795×10^{-2}	397.5
4	1.035×10^{-1}	450.0
5	2.760×10^{-1}	450.0
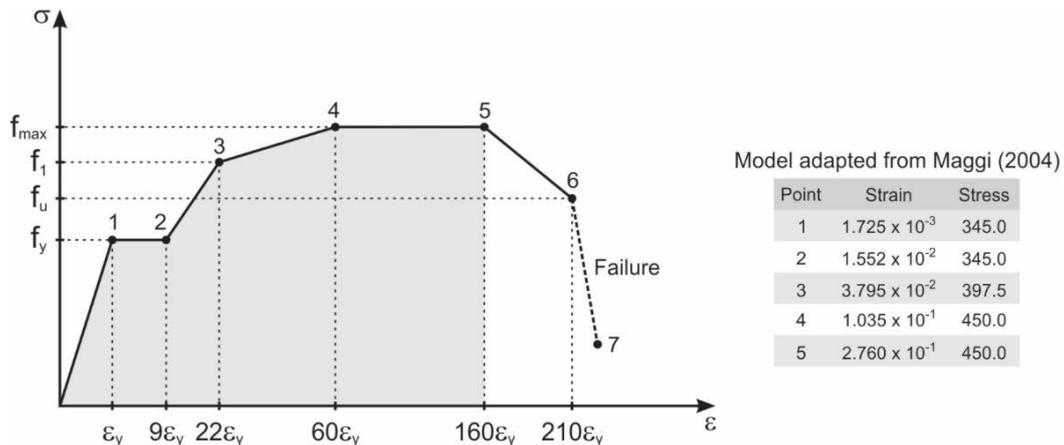
Fig. 6 Multilinear diagram of the steel behavior (adapted from Maggi 2004)

The Finite Element (FE) chosen to generate the mesh was SHELL181, which can be found in the library of ANSYS 16.0. This FE is suitable for analyzing thin to moderately thick shell structures. It is a four-node element with six degrees of freedom at each node: translation in the x, y and z directions, and rotations about the x, y and z-axes. The element formulation is based on logarithmic strain and true stress measures. The element kinematics allow the stretching of the finite membrane strains.

Fig. 5 portrays the geometry, node locations and the element coordinate system for this element, which is defined by a shell section and by four nodes (I, J, K and L). From the studies of Serrano-López *et al.* (2016), the finite element modelling with shell elements provides satisfactory and accurate results for a general purpose like a parametric study of the behavior of the joints analyzed in this work.

The adopted properties for the models were: yield stress equal to 345 MPa, ultimate tensile stress equivalent to 450 MPa, modulus of elasticity equal to 200 GPa and Poisson ratio of 0.3. Analyses were performed considering both physical and geometric nonlinearities, being the second one carried out by means of a model adapted from that proposed by Maggi (2004), as it can be

seen in Fig. 6. The complex statically undetermined frame structures would require the complete model with the softening response included, as it was stated by Imamovic *et al.* (2015) and Imamovic *et al.* (2018). However, the softening response (from point 5 to 7 of the following diagram) was not considered in this analysis, due to the numerical instability when considering the complete model proposed by Maggi (2004), as reported by Tristão (2006), Freitas (2009).

After setting the materials properties, the finite element mesh was generated from dividing each line segment shown in Fig. 7 into 10 equal parts. The beam-column joint needed to share the same mesh, in order to ensure the transmission of forces between the connected elements. Therefore, Fig. 8 shows the model with its already created meshes.

(a)   (b)
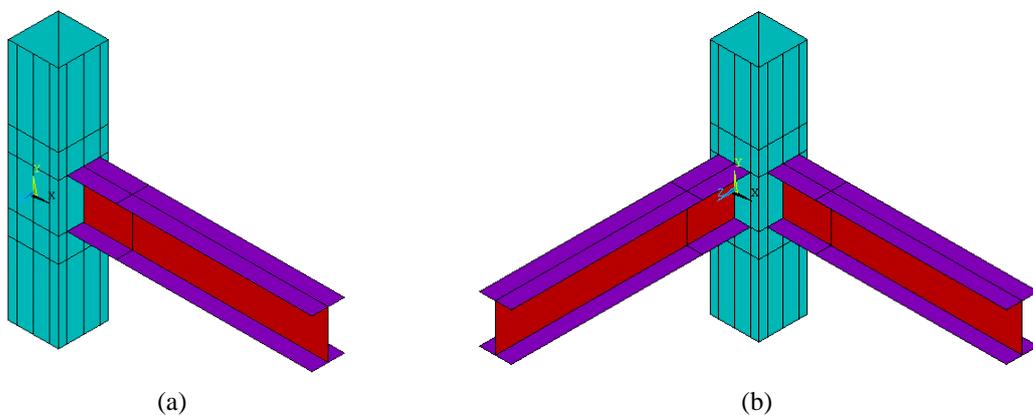
Fig. 7 Division of the meshes

(a)   (b)
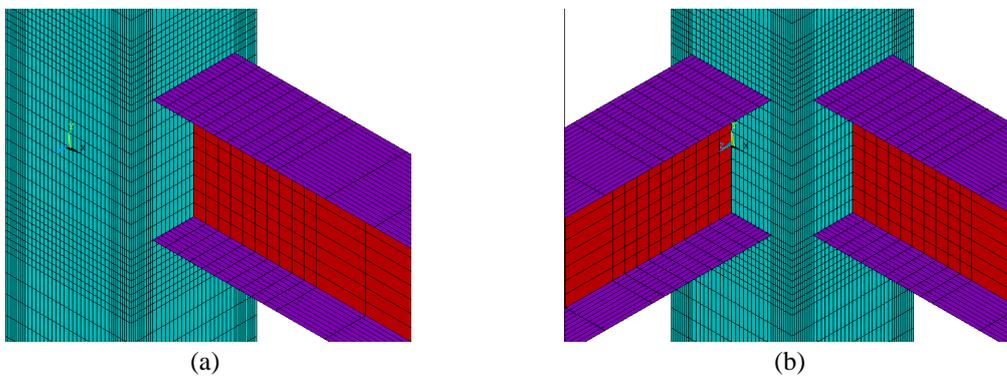
Fig. 8(a) uniplanar meshed model; (b) multiplanar meshed model

The application of boundary conditions consists in restricting all the six degrees of freedom in the nodes of the lower and upper extremities of the column, which will simulate fixed extremities. The following step was to apply a displacement of 50 mm in 100 increments at the end of the beams, with the aim of causing rotation in the welded connections and then plotting the moment-rotation curve.

The finite element mesh was generated in such way that model behaves as monolithic, which implies in using of the ANSYS 16.0 command glue to remove redundant nodes (i.e., repeated

Table 2 Geometric parameters

Model	Column	Beam	Geometric Parameters		
			β (b_1/b_0)	2γ (b_0/t_0)	η (h_1/b_0)
M1-U / M1-M	220x220x10	W200x15.0	0.45	22.00	0.91
M2-U / M2-M	220x220x10	W200x26.6	0.60	22.00	0.94
M3-U / M3-M	220x220x10	W200x41.7	0.75	22.00	0.93
M4-U / M4-M	220x220x16	W200x15.0	0.45	13.75	0.91
M5-U / M5-M	220x220x16	W200x26.6	0.60	13.75	0.94
M6-U / M6-M	220x220x16	W200x41.7	0.75	13.75	0.93
M7-U / M7-M	220x220x20	W200x15.0	0.45	11.00	0.91
M8-U / M8-M	220x220x20	W200x26.6	0.60	11.00	0.94
M9-U / M9-M	220x220x20	W200x41.7	0.75	11.00	0.93

Table 3 Analysis of the theoretical and numerical results for the resistant bending moment

Model	$M_{1,Rd}^{CIDECT}$	$M_{1,Rd}^{Lu}$	M_{num}^{Uni}	M_{num}^{Multi}	$\dfrac{M_{num}^{Uni}}{M_{1,Rd}^{CIDECT}}$	$\dfrac{M_{num}^{Uni}}{M_{1,Rd}^{Lu}}$	$\dfrac{M_{num}^{Multi}}{M_{1,Rd}^{CIDECT}}$	$\dfrac{M_{num}^{Multi}}{M_{1,Rd}^{Lu}}$	$\dfrac{M_{num}^{Multi}}{M_{num}^{Uni}}$
M1	36.40	33.10	96.39	90.91	2.6	2.9	2.5	2.7	0.9
M2	43.58	41.73	154.99	139.99	3.6	3.7	3.2	3.4	0.9
M3	53.81	55.79	204.84	204.85	3.8	3.7	3.8	3.7	1.0
M4	93.18	84.73	113.55	113.67	1.2	1.3	1.2	1.3	1.0
M5	111.57	106.84	209.21	183.20	1.9	2.0	1.6	1.7	0.9
M6	137.77	142.82	273.77	251.79	2.0	1.9	1.8	1.8	0.9
M7	145.60	132.39	116.49	115.75	0.8	0.9	0.8	0.9	1.0
M8	174.33	166.94	212.46	210.09	1.2	1.3	1.2	1.3	1.0
M9	215.26	223.15	278.01	288.90	1.3	1.2	1.3	1.3	1.0

nodes which share the same spatial coordinates with other nodes in the mesh). By using this strategy, the beam will be fixed in the column. Furthermore, numerical analyses were done according to the Newton-Raphson method, considering up to 15 iterations in each displacement increment.

4. Results and discussion

As seen previously in Table 1, it was considered two types of connections (uniplanar and multiplanar), three wall thickness for the RHS column and three I-beams profiles, which resulted in the analysis of eighteen different models, in order to evaluate the behaviour of the connections in different relations of stiffness. The geometric parameters that are required to determine the theoretical bending moment are presented in Table 2.

Table 3 shows the theoretical resistant bending moments, obtained by formulations recommended by Lu (1997) and CIDECT (2010), as well as compares these theoretical values with the numerical resistant bending moments, which were obtained from the non-convergent step

of the computational processing of each model. This non-convergent step characterizes the existence of regions of the models whose stresses reached the yielding stress. In the Table 3, M_{num}^{Uni} and M_{num}^{Multi} represent the numerical resistant bending moments of the uniplanar and multiplanar models, respectively. In the same way, $M_{1,Rd}^{CIDECT}$ and $M_{1,Rd}^{Lu}$ are the design resistant bending moment of the joints, which are established by CIDECT (2010) and Lu (1997), respectively.

It is observed from Table 3 that in the models formed by columns that have wall thickness of 10 mm, there was greater difference of the numerical results in relation to the analytical models of Lu (1997) and CIDECT (2010). On the other hand, for the connections involving columns that have wall thickness of 20 mm, there is greater similarity between these values. From the following table, it is noticed that there is a small variation among the resistant bending moments of the uniplanar and multiplanar models.

The ratios between numerical and theoretical resistant bending moment, illustrated in Table 3, are similar to those obtained by Nunes (2012), except for the models of this study with wall thickness of 10 mm. The studies of Nunes (2012) showed these ratios varying from 0.9 to 1.6.

The computational simulation was performed with the application of small increments of displacements at the ends of the beams, which allowed plotting the moment-rotation curve of each proposed model. Thus, these curves are shown in Fig. 9.
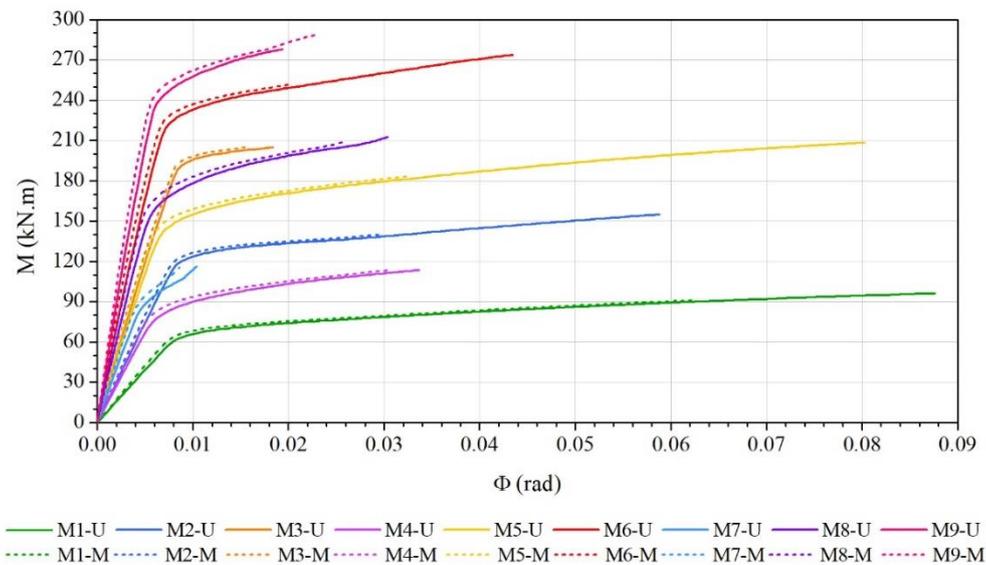

Fig. 9 Bending moment-rotation curves

According to the moment-rotation curves, presented in Fig. 9, it can be seen that the increase of the moment of inertia of the beam, using columns of the same wall thickness, decreases the rotation when submitted to a same bending moment, which indicates an improvement in the connection stiffness. Furthermore, the increase of the wall thickness of the column, when the same type of beam is used, increases the stiffness of the joint. The stiffness of the multiplanar models is a little higher than that of the uniplanar models, but this difference is insignificant.

The M7-U and M7-M models, composed by a tubular column that have wall thickness of

20 mm and one or two I-beams, highlight among the others models, since their moment-rotation curves have a different behaviour. So that to understand this difference, Fig. 10 shows the von Mises stresses of these models.

(a)   (b)
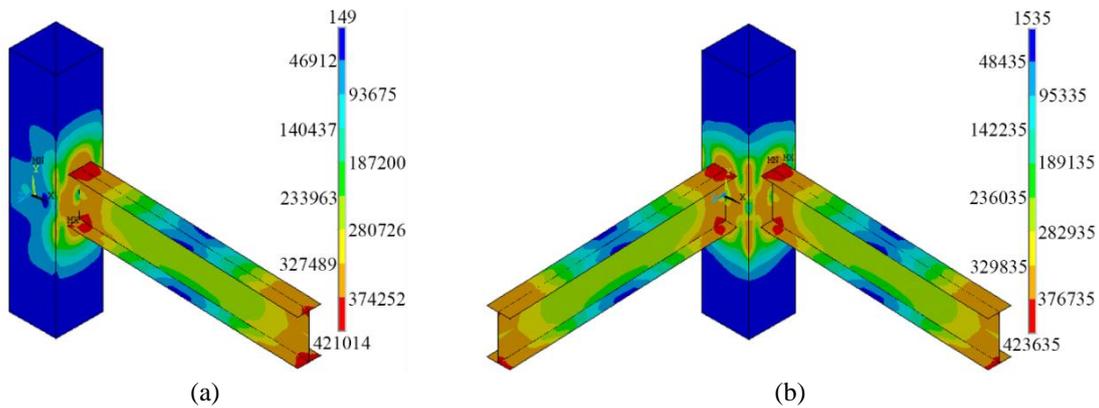
Fig. 10 von Miss stresses for (a) M7-U; (b) M7-M

From the previous figure, it can be identified that the higher stresses, of the M7-U and M7-M models, are located in the beam flange, in the regions close to the beam-column connection, which characterizes the local failure of the beam flange. However, the other models have higher stresses on the wall of the column, as it can be seen in Fig. 11, which shows the von Mises stresses of the M5-U and M5-M models. In addition, the other models present similar stress distributions to the ones presented in Fig. 11.

(a)   (b)
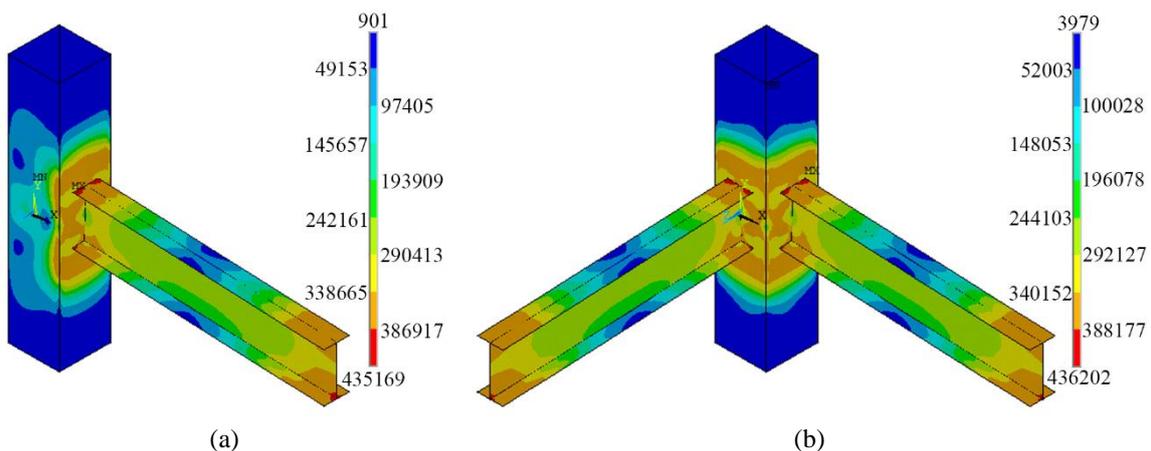
Fig. 11 von Miss stresses for (a) M5-U; (b) M5-M

Considering the analysis of the moment-rotation curves, it is possible to classify the connections according to their stiffness, taking into account the stiffness limits established by the

Table 4 Classification of the connections

| Model	Beam	I (cm^4)	Stiffness limits (kN m/rad)		Numerical stiffness (kN m/rad)		Classification
			S_{inf}	S_{sup}	$S_{uniplanar}$	$S_{multiplanar}$	
M1	W200x15.0	1,305.0	1,305.0	65,250.0	7,750.2	8,411.2	Semi-rigid
M2	W200x26.6	2,611.0	2,611.0	130,550.0	14,541.1	15,492.8	Semi-rigid
M3	W200x41.7	4,114.0	4,114.0	205,700.0	22,883.9	23,836.3	Semi-rigid
M4	W200x15.0	1,305.0	1,305.0	65,250.0	13,335.2	15,238.9	Semi-rigid
M5	W200x26.6	2,611.0	2,611.0	130,550.0	21,794.9	24,341.7	Semi-rigid
M6	W200x41.7	4,114.0	4,114.0	205,700.0	31,686.1	34,536.1	Semi-rigid
M7	W200x15.0	1,305.0	1,305.0	65,250.0	19,382.0	22,061.5	Semi-rigid
M8	W200x26.6	2,611.0	2,611.0	130,550.0	28,777.3	32,734.0	Semi-rigid
M9	W200x41.7	4,114.0	4,114.0	205,700.0	40,229.6	44,038.4	Semi-rigid
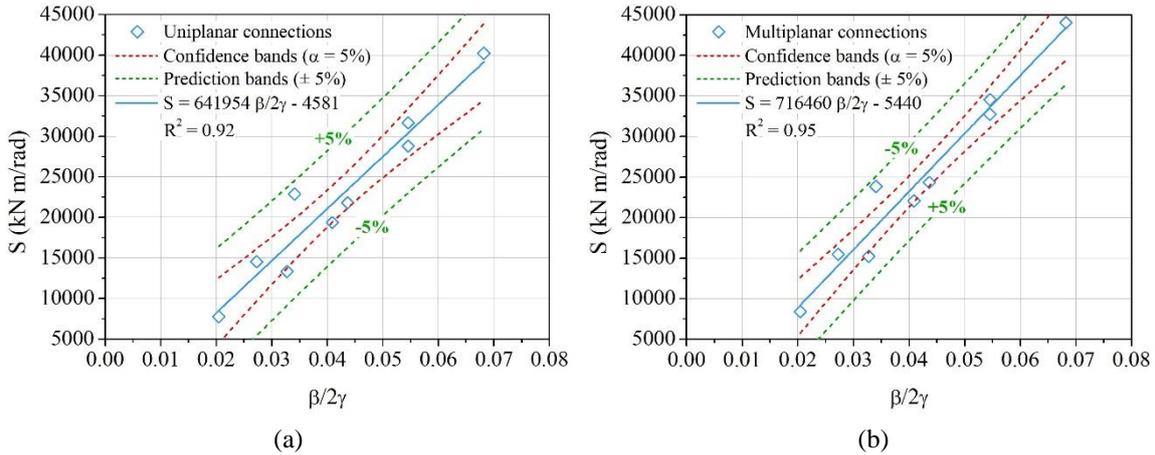
Fig. 12 (a) Uniplanar connections; (b) Multiplanar connections

Eurocode 3. Table 4 shows the limits of stiffness and the numerical stiffness of each connection. Those numerical stiffness are obtained from the tangent in the linear stretch of the M-φ curve, as it can be seen in Fig. 9. Therefore, all connections were classified as semi-rigid.

According to the studies of Nunes (2012), it was observed that the geometric parameters that most exert influence on stiffness are β and 2γ. Thus, the Stiffness versus β∕2γ graphs were plotted, in order to determine the expressions for the calculation of the connections stiffness, as it can be seen in Fig. 12, due to the possibility of generating trend lines, which allowed determining an equation for uniplanar connections and another for multiplanar connections, which are presented, respectively, in Eqs. (6) and (7).

$$S = 641954 \ \frac{\beta}{2\gamma} - 4581 \tag{6}$$

$$S = 716460 \ \frac{\beta}{2\gamma} - 5440 \tag{7}$$

5. Conclusions

The numerical results are more similar to the theoretical prescriptions predicted by CIDECT (2010), especially for the models constituted by tubular columns with thickness of 16 mm and 20 mm. Moreover, this study revealed that uniplanar and multiplanar connections have similar behavior, since these connections have similar bending moment strength and stiffness. However, the stiffness of the multiplanar models is a little bit higher than that one of the uniplanar models. So, the theoretical prescriptions, proposed for uniplanar welded connections, are suitable for the development of structural projects that have multiplanar connections.

As shown in the plotted moment-rotation curves, the increase of the moment of inertia of the beam, using columns of the same wall thickness, causes an improvement in the connections stiffness. Besides this improvement, the increase of the wall thickness of the column, when a same type of beam is used, raises the stiffness of the joint. Therefore, the inertia of the beam and column influences the stiffness of the welded connections.

The M7-U and M7-M models presented a failure mode different from the others, considering the fact that their failure mode originated cracks in the beam flange. On the other hand, the other models presented a column wall plastification at the beginning of this study.

In this study, all the connections proposed were classified as semi-rigid, from the limits established by Eurocode 3. This fact indicates the importance of considering the real stiffness of the connection in the projects, so that it results in an economic project. Then, this study proposed two equations to estimate the stiffness of uniplanar and multiplanar welded connections, in which their coefficients of determination are equal to 0.92 and 0.95, respectively.

The low amount of models studied in this research is considered as a limitation of the analysis. Therefore, it is vital to emphasize the need of carrying out more researches about this subject, which will enable a better understanding of the behaviour of this type of connection.

References

Ansys, Inc (2015), *Theory Reference (Version 16.0)*.

Díaz, C., Martí, P., Victoria, M. and Querin, O.M. (2011), "Review on the modelling of joint behaviour in steel frames", *J. Constr. Steel Res.*, **67**(5), 741-758.

EN 1993-1-8 (2005), *Eurocode 3: Design of Steel Structures-Part 1-8: Design of Joints*, European Committee for Standardization, Brussels, Belgium.

Eslami, M. and Namba, H. (2016a) "Mechanism of elasto-plastic behavior of composite beam connected to RHS column", *Int. J. Steel Struct.*, **16**(3), 913-933.

Eslami, M. and Namba, H. (2016b) "Elasto-plastic behavior of composite beam connected to RHS column, experimental test results", *Int. J. Steel Struct.*, **16**(3), 901-912.

Faridmehr, I., Tahir, M.M. and Lahmer, T. (2016), "Classification system for semi-rigid beam-to-column connections", *Lat. Am. J. Sol. Struct.*, **13**(11), 2152-2175.

Freitas, P.C.B. (2009), "Análise numérica de ligações metálicas viga-coluna com coluna tubular circular", M.Sc. Dissertation, University of São Paulo, São Carlos, Brazil.

Guerra, M.J.L., Reis, S.L.F., Nunes, G.V. and Sarmanho, A.M. (2013), "Análise da rigidez de ligações metálicas soldadas entre pilar de seção RHS e viga de seção I", *Proceedings of the 34th Ibero-Latin American Congress on Computational Methods in Engineering*, Pirenópolis, Brazil, November.

Imamovic, I., Ibrahimbegovic, A. and Mesic, E. (2018), "Coupled testing-modeling approach to ultimate state computation of steel structure with connections for statics dynamics", *Coupled Syst. Mech.*, **7**(5), 555-581.

Imamovic, I., Ibrahimbegovic, A., Knopf-Lenoir, C. and Mesic, E. (2015), "Plasticity-damage model parameters identification for structural connections", *Coupled Syst. Mech.*, **4**(4), 337-364.

Lozano, M., Serrano, M.A., López-Colina, C., Gayarre, F.L. and Suárez, J. (2018), "The influence of the heat-affected zone mechanical properties on the behaviour of the welding in transverse plate-to-tube joints", *Mater.*, **11**(2), 266.

Lu, L.H. (1997), "The static strength of I-beam to rectangular hollow section column connections", Ph.D. Dissertation, Delft University, the Netherlands.

Machado, R.B. (2013), "Análise numérica e experimental de ligações soldadas na direção de menor inércia do pilar", Ph.D. Dissertation, Federal University of Ouro Preto, Ouro Preto, Brazil.

Maggi, Y.I. (2004), "Análise do comportamento estrutural de ligações parafusadas viga-pilar com chapa de topo estendida", Ph.D. Dissertation, University of São Paulo, São Carlos, Brazil.

Matos, R.M.M.P., Costa-Neves, L.F., Lima, L.R.O., Vellasco, P.C.G.S. and Silva, J.G.S. (2015), "Resistance and elastic stiffness of RHS "T" joints: Part I-axial brace loading", *Lat. Am. J. Sol. Struct.*, **12**(11), 2159-2179.

Nunes, T.C. (2012), "Análise de ligações metálicas soldadas entre pilar de seção RHS e viga de seção I", M.Sc. Dissertation, Federal University of Ouro Preto, Ouro Preto, Brazil.

Rocha, B.S. and Neto, J.G.R. (2016), *Análise de Ligações Soldadas entre Vigas de Seção I e Pilares em Perfis Tubulares*, Revista Interdisciplinar de Pesquisa em Engenharia.

Serrano-López, M.A., López-Colina, C., González, J. and López-Gayarre, F. (2016), "A simplified FE simulation of welded I beam-to-RHS column joints", *Int. J. Steel Struct.*, **16**(4), 1095-1105.

Wardenier, J., Packer, J.A., Zhao, X.L. and Van der Vegte, G.J. (2010), *Hollow Sections in Structural Applications*, 2nd Edition, CIDECT, Geneva, Switzerland.

Wu, J. and Feng, Y.T. (2013), "Finite element simulation of new RHS column-to-I beam connections for avoiding tensile fracture", *J. Constr. Steel Res.*, **86**, 42-53.

AI